

Condensed Matter and Interphases

Kondensirovannye Sredy i Mezhfaznye Granitsy
<https://journals.vsu.ru/kcmf/>

Original articles

Research article

<https://doi.org/10.17308/kcmf.2023.25/11261>

Hydrogen permeability of 48Cu52Pd cold-rolled alloy foil and different methods of its surface pretreatment

N. B. Morozova¹✉, L. E. Sidiyakina¹, A. I. Dontsov^{1,2}, A. V. Vvedenskii¹

¹Voronezh State University,
1 Universitetskaya pl., Voronezh 394018, Russian Federation

²Voronezh State Technical University,
20 letiya Oktyabrya st., 84, Voronezh 394006, Russian Federation

Abstract

The process of atomic hydrogen penetration into the metal phase is complicated by the phase-boundary transition from the liquid and/or gas phase. That is why the cleanliness of metal and alloy surfaces is of particular importance. The purpose of this work was to determine the effect of surface pretreatment using photon pulses, ultrasound, and potential cycling on the parameters of hydrogen permeability for 48Cu52Pd metal cold-rolled membranes.

The study was focused on a foil of copper-palladium homogeneous alloy with 48 at. % Cu and 52 at. % Pd composition. The studied samples were obtained by cold rolling and their thickness were 10 and 16 μm . Surface pretreatment included rinsing in acetone, using ultrasound, pulsed photon treatment, and quadruple potential cycling over a wide range of potentials. Electrochemical studies included cyclic voltammetry and cathode-anodic chronoamperometry in a deaerated 0.1 M H_2SO_4 solution. Hydrogen permeability was calculated using mathematical models for samples of finite and semi-infinite thickness.

It was found that the surface treatment of a 48Cu52Pd foil with photon pulses leads to both an increase in the ionisation rate of atomic hydrogen and an increase in the roughness of the foil surface. The diffusion coefficient of atomic hydrogen does not depend on the method of surface pretreatment with ultrasound and photon pulses. The extraction rate constant for the extraction of the atomic hydrogen after photon treatment increases, which facilitates the processes of both H introduction and ionisation due to the release of active centres of the surface. Electrochemical cleaning of the surface during the quadruple potential cycling contributes to the growth of the extraction rate constant for the extraction of atomic hydrogen.

Keywords: 48Cu52Pd foil, Cold rolling, Hydrogen permeability, Surface pretreatment, Pulsed photon treatment, Ultrasound

Funding: The work was supported by the Ministry of Science and Higher Education of the Russian Federation in the framework of the government order to higher education institutions in the sphere of scientific research for years 2023-2025, project No. FZGU-2023-0006.

For citation: Morozova N. B., Sidiyakina L. E., Dontsov A. I., Vvedenskii A. V. Hydrogen permeability of 48Cu52Pd cold-rolled alloy foil and different methods of its surface pretreatment. *Condensed Matter and Interphases*. 2023;25(3): 373–382. <https://doi.org/10.17308/kcmf.2023.25/11261>

Для цитирования: Морозова Н. Б., Сидякина Л. Е., Донцов А. И., Введенский А. В. Водородопроницаемость фольги из холоднокатанных сплавов 48Cu52Pd с различной предобработкой поверхности. *Конденсированные среды и межфазные границы*. 2023;25(3): 373–382. <https://doi.org/10.17308/kcmf.2023.25/11261>

✉ Natalia B. Morozova, e-mail: mnb@chem.vsu.ru

© Morozova N. B., Sidiyakina L. E., Dontsov A. I., Vvedenskii A. V., 2023



The content is available under Creative Commons Attribution 4.0 License.

1. Introduction

The production of high-purity hydrogen is important not only for hydrogen energy engineering, but also for hydraulic cleaning, hydrocracking, the production of synthetic fuel, etc. [1]. Various materials, such as polymers, zeolites, carbon, and certain metals, have previously been investigated for the purpose of obtaining high-quality membranes to isolate H₂ from a mixture with other gases [2], however, most of these membranes have low selectivity. Palladium-based membranes have high permeability and selectivity to molecular hydrogen due to a high dissociation rate and a high rate of atomic hydrogen penetration into the metal phase [3]. The main requirement for such membranes is their ability to prevent surface fouling with sulphur and its compounds. For this, copper, gold, and silver are added to palladium, both individually and in various combinations [4–6].

In particular, Pd-Cu membranes are recognised as the most promising due to their relatively low cost, noticeable resistance to fouling, and higher hydrogen permeability as compared to other Pd-based membranes [5,7–10]. Over the entire concentration range, Pd-Cu crystalline alloys are a continuous series of solid solutions [11]. However, the Cu-Pd alloy with a palladium content of 47 at. % demonstrates the highest hydrogen permeability [12]. It is also cost-effective as the copper content is just over 50 at. % [5]. Such an alloy is characterised by a sharp maximum of hydrogen permeability and forms the β -phase of a Pd-Cu solid solution at equilibrium. It was noted [9] that despite the same ratios of components in the alloy, due to its dense structure its high-temperature phase with the FCC lattice (α -phase) demonstrates a significantly lower hydrogen permeability than the β -phase.

The process of the atomic hydrogen penetration into the metal phase is complicated by the phase-boundary transition from the liquid and/or gas phase [13], therefore, there are additional requirements for the cleanliness of metal and alloy surfaces. This is especially important when using metal membranes obtained by cold rolling. In particular, organic oils used during rolling considerably pollute the surface of the metal

phase, which inhibits the penetration of atomic hydrogen into the metal. In addition, oils can form durable polymer films on the surface. When manufacturing thin membranes whose thickness is just several microns, mechanical cleaning of their surfaces is absolutely unacceptable. What is more, when alloy membranes are used, chemical etching is also out of question.

The most common safe methods for preparing surfaces of metal samples that can be used for alloys include: laser [14, 15] and ultrasonic [16, 17] cleaning, high-temperature annealing [18, 19], and electrochemical cleaning [20]. Most physical cleaning methods are quite effective at removing persistent surface contamination, however, excessive cleaning intensity results in surface damage. Whereas, the method of electrochemical cleaning allows, by selecting the potential and the optimal number of cycles, removing substances of different solubility from the surface of noble metals and alloys based on them without changing the surface morphology [21].

The purpose of this work was to determine the effect of surface pretreatment using photon pulses, ultrasound, and potential cycling on the parameters of hydrogen permeability for 48Cu52Pd metal cold-rolled membranes.

2. Experimental

The study was focused on a copper-palladium foil with a thickness l and a composition of 48 at. % Cu and 52 at. % Pd, which was obtained by cold rolling*. The surface of the foil was pretreated by different methods. The pretreatment conditions included rinsing in acetone (30 min) in an ultrasonic bath (ODA-LQ07 (Russia)) at an operating frequency of 40 kHz. This was followed by pulsed photon treatment (PPT) at a radiation energy of $\sim 35 \text{ J}\cdot\text{cm}^{-2}$ using a UOLP-1 unit, in a vacuum of 10^{-3} Pa using powerful INP 16/250 pulse xenon lamps (radiation spectrum 0.2–1.2 μm), and subsequent annealing in a vacuum at 350 °C.

The thickness of the samples and the methods used for surface pretreatment are shown in Table 1.

Electrochemical measurements were taken using an IPC-Compact potentiostat. The working

* The samples of palladium alloys were produced at the Baikov Institute of Metallurgy and Materials Science.

Table 1. Studied objects and method of their surface treatment

Sample	$l, \mu\text{m}$	Pretreatment method		
		Acetone	US (30 min)	PPT duration, s ; $I = 50 \text{ A}$
1	16	+	+	–
2	10	+	+	1.0·10 (one side)
3	10	+	+	0.7·10 (two side)
4	10	+	+	0.7·10 (one side)

electrode was a sample of a 48Cu52Pd metal foil attached with a conductive graphite adhesive to a spectrally pure graphite electrode. The studies were carried out in a deaerated 0.1M H_2SO_4 solution (extra-pure grade) in a three-electrode cell with anode and cathode spaces separated with a thin section. A copper-sulphate electrode ($E = 0.298 \text{ V}$) was used as the reference electrode. The auxiliary electrode was a platinised platinum Pt(Pt) electrode. All potentials were recalculated relative to a standard hydrogen electrode and the current values were given per single unit of the visible surface. The area of the studied foil samples did not exceed 0.5 cm^2 .

The methods included cyclic voltammetry and two-stage anodic-cathodic chronoamperometry.

Voltammograms (VAG) were obtained from preliminary quadruple cycling of the working electrode within the potential range from $E_c = -0.27 \text{ V}$ to $E_a = 1.70 \text{ V}$ with a scanning rate of 5 mV/s . Before cycling and between cycles, the electrode was pre-polarised in a working solution at a potential of $E_{pp} \approx 0.30 \text{ V}$ for $t_{pp} = 500 \text{ s}$. The electrode was not removed from the solution. It was found that an increase in the number of cycles did not lead to any significant changes in the shape of voltammograms.

The method of cyclic voltammetry also determined the ionisation potential of atomic hydrogen E_p as the peak potential of hydrogen ionisation in the fourth cyclogram. The value E_p was used to obtain the anode half-period of the chronoamperogram. It should be noted that the values of E_p slightly differed due to the heterogeneity of the alloy surface after rolling.

Before obtaining the i, t -dependences, the electrode was pre-polarised at a potential of $E_{pp} \approx 0.30 \text{ V}$, which corresponded to the values of cathodic current not exceeding $2\text{--}4 \mu\text{A}$. Chronoamperograms were obtained at the cathode hydrogenation potential $E_c = -0.08 \text{ V}$ for t_s from 1 to 10 s, and the anode ionisation

potential E_p for $t_a = 500 \text{ s}$. The cathode half-period of the chronoamperogram characterised the process of atomic hydrogen injection, while the anode half-period described its extraction. The time of the sample hydrogenation was chosen to prevent the formation of the palladium hydride β -phase within the metal phase. Over $t_s = 10 \text{ s}$, the α -phase of the Pd-H solid solution was formed in the alloy, which was characterised by the ratio $\text{H/Pd} = 0.02$. We assumed that recharging of the double electric layer took little time, therefore, the anodic current transient i_a , which was observed for at least 500 s, was mainly due to the Faraday effect on the ionisation of atomic hydrogen.

Micrographs of the studied samples were obtained using a Solver P47PRO atomic force microscope (Russia) in a semi-contact (intermittent-contact) scanning mode.

3. Results and discussion

2.1. Analysis of cyclic voltammograms and chronoamperograms

Cyclic voltammograms obtained during quadruple cycling of the studied samples are shown in Fig. 1. They are characterised by two main peaks. The peak on the anodic branch of the curve corresponded to the ionisation of atomic hydrogen at $E \sim 0.2\text{--}0.4 \text{ V}$, while the peak on the cathodic branch at $E \sim 0.55 \text{ V}$ corresponded to the PdO reduction [22]. The absence of ionisation peaks on samples 1 and 3 during the first cycle indicated that the active centres on the surface remained blocked even after the application of ultrasound and the PPT. Therefore, the pre-treatment procedure used for these samples was not effective. It can be assumed that oil annealing products used during alloy rolling were not removed completely. Within the potential range from 1.1 to 1.3 V, a blurred electrooxidation (EO) peak was observed on the anodic branch of the curve, which could be

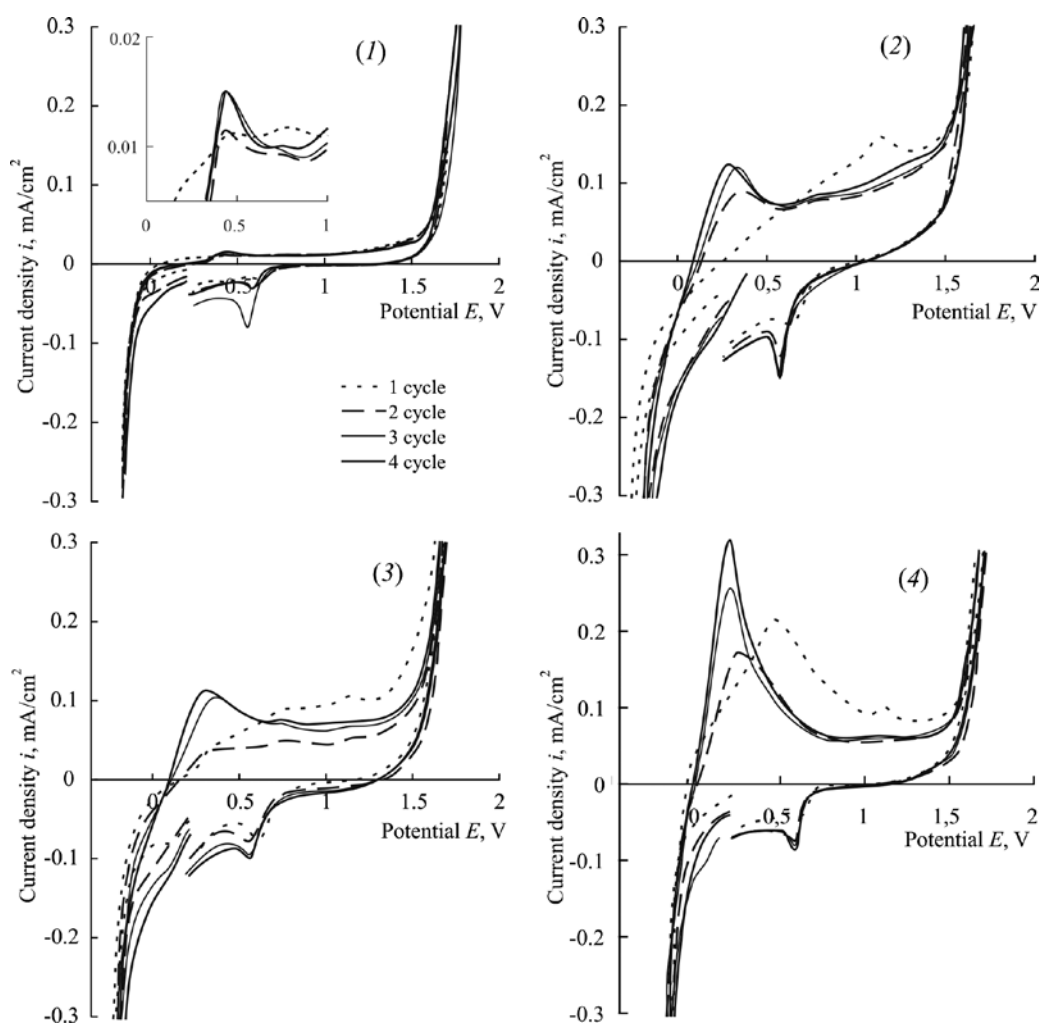


Fig. 1. Cyclic current-voltage curves with four-fold scanning of the potential of samples 1-4 of 48Cu52Pd alloy obtained in a 0.1M H₂SO₄ solution with a scanning rate of 5 mV/s

associated with the oxidation of traces of organic oils on the surface. However, in subsequent cycles, this peak was noticeably suppressed and, as a result, an ionisation peak of atomic hydrogen either appeared (samples 1, 3) or increased (samples 2, 4).

To find the parameters for the processes of introduction and ionisation of atomic hydrogen, two-stage cathodic-anodic chronoamperograms were obtained. For all chronoamperograms, the time of sample hydrogenation was $t_c = 10$ s. Both cathodic and anodic current transients in all samples were of the same nature. Cathodic current transients demonstrated a sharp decrease in the extraction rate in the first 3–4 seconds. For sample 4, there was a sharper transients than for samples 1-3. Anodic current transients also had a clear peak of H ionisation current, which

decreased nonlinearly and completed a sharp decline after the first 10 s (Fig. 2).

The highest ionisation rates were observed in the fourth sample, and the lowest ionisation rates were in the first sample, which means that the PPT plays a significant role in eliminating oil products left after rolling and subsequent annealing of the sample. The comparison of the obtained results revealed that the highest ionisation rate was observed for the foil of the fourth sample, which had been rinsed in acetone and one side of which was exposed to ultrasound and photon treatment. The lowest ionisation peak was characteristic of the sample which hadn't been exposed to the PPT. Therefore, photon treatment of the surface contributed significantly to the surface cleaning of palladium and copper alloy samples after rolling and this effect was

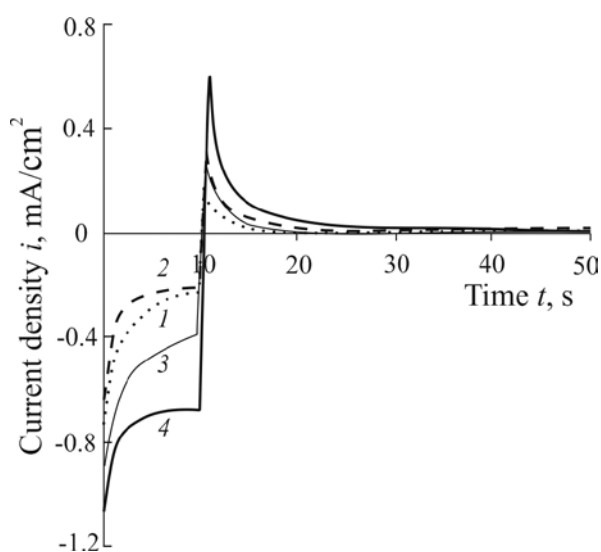


Fig. 2. Combined cathodic and anodic chronoamperograms of the studied samples (1-4) of 48Cu52Pd alloy obtained in a 0.1M H₂SO₄ solution after quadruple cycling at $t_c = 10$ s

noticeable in all samples which had been exposed to photon irradiation.

2.2. Microscopic examination of sample surfaces

The geometrical characteristics of the surfaces of 48Cu52Pd alloys both before and after the PPT were determined using atomic force microscopy (AFM). When comparing micrographs (Fig. 3), it can be seen that the PPT led to the appearance of globules on the surfaces of samples whose size reached ~700 nm. The globules were located

on an initially even surface, which allows us to assume that they were formed as a result of the alloy’s redeposition after the PPT procedure. The presence of these particles led to an increase in the total surface area of the studied samples. Also, the micrographs made before the PPT clearly showed the grain boundaries of the alloy, whose diameter was about 15–20 μm .

According to the results of AFM, the roughness of the alloy surface after the PPT increased by 3–5 times. It can be assumed that pulsed photon treatment of the surface not only removed the oil products used during rolling, but also led to the alloy redeposition being accompanied by the formation of globules. This resulted in the development of the alloy surface.

An increase in the rate of hydrogen ionisation on alloys after the PPT can also be associated with an increase in the surface area of the samples. However, even a five-fold increase (if we compare the peak heights of voltammograms of sample 1 without the PPT and samples 2–4) did not produce the results obtained for samples 2–4. This means that an increase in the rate of hydrogen ionisation should be associated not so much with an increase in the surface area of the alloy, but with a change in the state of its surface layer.

2.3. Calculating the parameters of hydrogen permeability

Two models for determining the parameters of hydrogen permeability were used to process

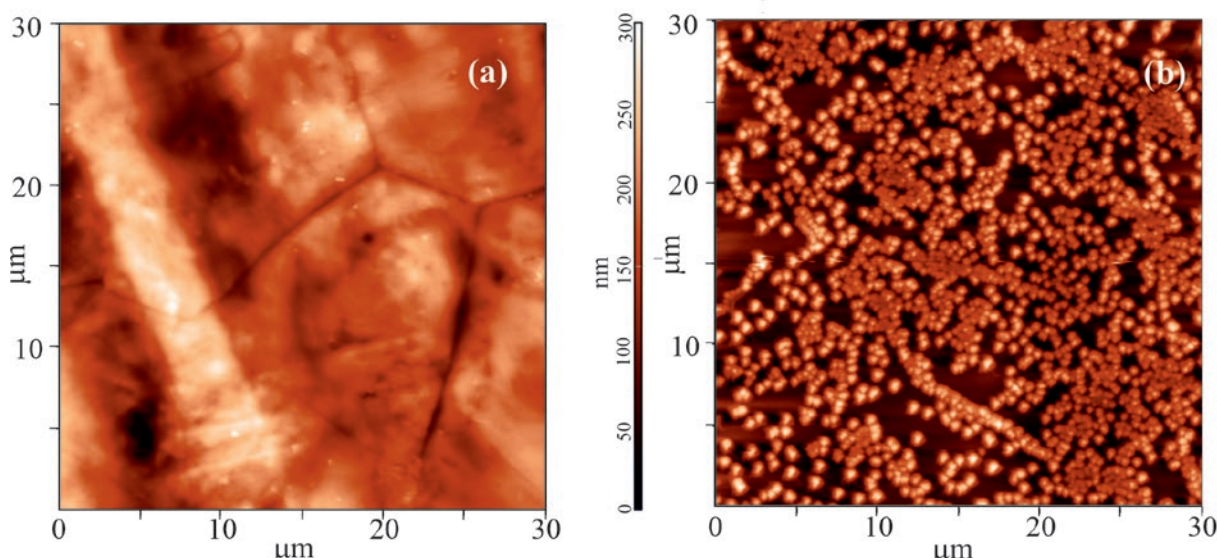


Fig. 3. AFM micrographs obtained for 48Cu52Pd alloy before (a) and after (b) the PPT

i, t -curves. The first model was valid for samples of semi-infinite thickness [13], for which the period of hydrogenation of 10 s was not enough for atomic hydrogen to cross the studied sample. Its application adequately described the processes of the introduction and ionisation of atomic hydrogen in samples with a thickness of more than 10 μm . The second model was applicable for samples of finite thickness which did not exceed 10 μm [24].

Since the thickness of sample 1 was 16 μm , we used the first model to calculate the parameters of hydrogen permeability. While the model of thin electrodes was used to process the current transients obtained for samples 2–4. This means that it was not possible to calculate the diffusion coefficient D_{H} for the first sample. For it, we could only determine a complex parameter, namely the hydrogen permeability coefficient K_{D} , which included the diffusion coefficient and the change in the concentration of atomic hydrogen in the film relative to its equilibrium value Δc_{H} :

$$K_{\text{D}} = \sqrt{D_{\text{H}}} \cdot \Delta c_{\text{H}}. \quad (1)$$

The cathodic chronoamperograms revealed two areas of current transients. One was located at initial times $t \leq 3$ s, while the second was located at times $t > 4$ s. In the initial period of time, the stage that determined the rate was the stage of atomic hydrogen transition through the solution/metal interphase. Therefore, at the initial section, there was a phase-boundary control of the process of the atomic hydrogen introduction, which for electrodes with $l > 10 \mu\text{m}$ was described by equation [13]:

$$i_{\text{c}}(t) = i_{\text{c}}(0) - [i_{\text{c}}(0) - i_{\text{c}}^{\infty}] \cdot \frac{2\bar{k}}{\pi^{1/2} \cdot D_{\text{H}}^{1/2}} \cdot t^{1/2}, \quad (2)$$

and for samples with $l < 10 \mu\text{m}$ by equation [23]:

$$\ln[i_{\text{c}}(t) - i_{\text{c}}^{\infty}] = \ln(F\bar{k}\Delta c_{\text{H}}) - \frac{\bar{k}t}{l}. \quad (3)$$

Here, $i_{\text{c}}(0)$ and i_{c}^{∞} are the initial and stationary cathodic currents of the chronoamperograms, respectively, and \bar{k} is the effective constant of the H extraction rate.

When hydrogenation times exceeded 4 s, the control was passed to the stage of solid-phase diffusion, and for samples with $l > 10 \mu\text{m}$ it was described by the equation:

$$i_{\text{c}}(t) = i_{\text{c}}^{\infty} + \frac{FK_{\text{D}}}{\pi^{1/2}t^{1/2}}, \quad (4)$$

whereas for samples with $l < 10 \mu\text{m}$ it was described by the equation:

$$\ln[i_{\text{c}}(t) - i_{\text{c}}^{\infty}] = \ln\left(\frac{2FD}{l} \Delta c_{\text{H}}\right) - \frac{2D_{\text{H}}t}{l^2}. \quad (5)$$

The parameters of hydrogen permeability determined by anodic current transients were also calculated using two mathematical models. However, due to a more complex mathematical solution of the equation describing the complete curve of anodic current transients, it was only possible to quantitatively consider the case of mixed phase-boundary diffusion kinetics. In that case, we considered sections of anodic chronoamperograms obtained at $t > 30$ s. Then, in models for electrodes of both semi-infinite and finite thickness, the linearisation equations for anodic current transients were as follows:

- for electrodes with $l > 10 \mu\text{m}$

$$i_{\text{a}}(t) = i_{\text{a}}^{\infty} - \frac{FK_{\text{D}}}{\pi^{1/2}} \left(\frac{1}{(t-t_{\text{c}})^{1/2}} - \frac{1}{t^{1/2}} \right); \quad (6)$$

- for electrodes with $l < 10 \mu\text{m}$

$$\ln\left(\frac{i_{\text{a}}(t) - i_{\text{a}}^{\infty}}{i_{\text{a}}(t_{\text{c}}) - i_{\text{a}}^{\infty}}\right) \approx -\frac{\pi^2 D_{\text{H}}(t-t_{\text{c}})}{4l^2}. \quad (7)$$

Here, $i_{\text{a}}(t_{\text{c}})$ and i_{a}^{∞} are the initial and stationary anodic currents of the chronoamperograms, respectively.

Under these conditions, linearisation equations (2)–(7) could only be used to calculate the parameters D_{H} and Δc_{H} for thin samples, and parameter K_{D} for sample 1, which were found by the value of the slopes of the linearised dependencies. The obtained parameters are shown in Table 2.

It is important to note that surface treatment with photons pulses had nearly no effect on the diffusion coefficient of samples 2–4, which was primarily determined by the structural and chemical composition of the alloy. However, the concentration of atomic hydrogen in the alloy decreased linearly with a decrease in the irradiation intensity during the transition from the second sample to the fourth both at the initial stage, when phase-boundary control was

Table 2. Values of the parameters of hydrogen permeability calculated by cathodic and anodic chronoamperograms under kinetics with different controls

Sample		1	2	3	4	
Cathodic process	Diffusion control	$D_H \cdot 10^8, \text{cm}^2/\text{s}$	–	3.24 ± 1.96	4.33 ± 0.69	3.83 ± 0.11
		$\Delta c_H \cdot 10^5, \text{mol}/\text{cm}^3$	–	5.26 ± 1.95	4.06 ± 0.05	2.48 ± 0.53
	Phase boundary control	$\bar{k} \cdot 10^4, \text{cm}/\text{s}$	3.16 ± 0.05	4.66 ± 1.51	5.12 ± 0.78	6.74 ± 1.41
		$\Delta c_H \cdot 10^5, \text{mol}/\text{cm}^3$	–	1.93 ± 0.94	1.48 ± 0.48	1.02 ± 0.25
	$K_D \cdot 10^9, \text{mol}/\text{cm}^2 \cdot \text{s}^{1/2}$	6.24 ± 0.05	8.90 ± 0.54	6.68 ± 0.63	4.86 ± 1.02	
Anodic process	$D_H \cdot 10^8, \text{cm}^2/\text{s}$	–	1.02 ± 0.01	1.70 ± 0.20	1.34 ± 0.07	
	$\Delta c_H \cdot 10^5, \text{mol}/\text{cm}^3$	–	0.44 ± 0.20	0.32 ± 0.21	1.69 ± 1.13	
	$K_D \cdot 10^9, \text{mol}/\text{cm}^2 \cdot \text{s}^{1/2}$	0.39 ± 0.11	0.44 ± 0.08	0.42 ± 0.12	1.70 ± 0.21	

implemented, and at longer times, when diffusion control dominated.

The value of the effective constant of the extraction rate of atomic hydrogen, on the \bar{k} contrary, increased. Since the rate constant characterises the phase-boundary transition of H and surface processes, in particular, the extraction of atomic hydrogen from the alloy, it must be sensitive to the surface cleanliness. This means the higher \bar{k} , the cleaner the surface should be, therefore, the surface was cleaned during the transition from sample 1 to sample 4. The obtained data explain an increase in the ionisation peak in voltammograms and the presence of maximum ionisation currents in chronoamperograms during the transition from sample 1 to sample 4. The hydrogen permeability constant K_D changed in the same way as the concentration of atomic hydrogen in the alloy. However, for sample 1, the hydrogen permeability was lower than for samples 2 and 3 and higher than for sample 4.

According to (1), the concentration of atomic hydrogen contributed more to the value K_D rather than its diffusion coefficient. The comparison of the obtained results for cathodic and anodic current transients revealed that the values of the diffusion coefficient D_H determined by anodic transients were almost twice smaller than for the cathodic transients. This may be due to the fact that part of atomic hydrogen was captured in trap defects of the alloy, that is why the time of the experiment (500 s) did not allow completely extracting all the injected atomic hydrogen.

2.4. The role of electrochemical pretreatment of the surface

Suppression of the anodic peak of electrooxidation during the transition from the first to the fourth cycle of voltammograms (Fig. 1) occurred as a result of multiple cycling of the electrode potential. Therefore, it is interesting to understand the role of electrochemical surface pretreatment in the overall cleaning procedure. For this study, we chose the sample with the highest atomic hydrogen ionisation rate, i.e. sample 4. Chronoamperograms were obtained for this sample without preliminary quadruple potential cycling and after the cycling (Fig. 4). Sample 4 that had not been exposed to preliminary cycling was designated as 4'.

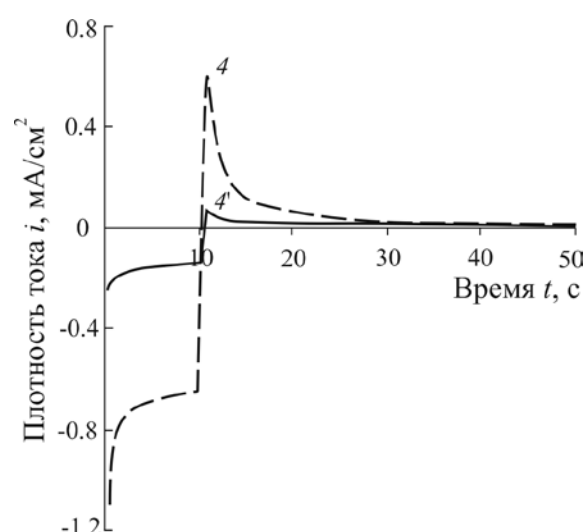


Fig. 4. Chronoamperograms for 48Cu52Pd alloy sample 4 obtained in a 0.1M H_2SO_4 solution without (4') and after preliminary quadruple potential cycling (4)

The comparison of the i, t -curves obtained for sample 4' with the curves obtained for sample 4 revealed that the introduction rate was about 5 times lower and the ionisation rate was almost 10 times lower. For these samples, we only calculated the parameters of hydrogen permeability by cathodic current transients since they are more informative.

The comparison of parameters calculated for samples 4' and 4 showed that the diffusion coefficient of atomic hydrogen for both samples coincided within the limits of experimental error (Table 3). However, the extraction rate constant decreased by almost 2 times, which suggests that the phase-boundary transition for the alloy without electrochemical pretreatment was inhibited. The concentration of atomic hydrogen in the alloy both at the stage of phase-boundary exchange and at the diffusion stage decreased. However, the concentration of H at the stage of phase-boundary exchange decreased to a greater extent for the sample which had not been exposed to preliminary potential cycling. In our opinion, this can be due to inhibited process of the atomic hydrogen penetration through the metal/solution interface. Sample 4' was characterised by lower values of the parameters of hydrogen permeability, except for the diffusion coefficient.

4. Conclusions

1. The methods of voltammetry and chronoamperometry allowed establishing that for the foil made from a cold-rolled 48Cu52Pd alloy, surface treatment with photon pulses leads to an increase in the ionisation rate of atomic hydrogen by 15–25 times depending on the sample. This results in the cleaning of the sample surface and in an increase of its roughness (3–5 times), which most likely happens due to the redeposition of the alloy during photon treatment.

2. The diffusion coefficient of atomic hydrogen for samples with a thickness of $l = 10 \mu\text{m}$ is about $4 \cdot 10^{-8} \text{ cm}^2/\text{s}$ and does not depend on the method of surface pretreatment with ultrasound and photon pulses. However, extraction rate constant for the extraction of the atomic hydrogen, which characterises the rate of the phase-boundary transition, slightly increases during the transition from sample 1 to sample 4 from $3.16 \cdot 10^{-4}$ to $6.74 \cdot 10^{-4} \text{ cm/s}$, respectively. This fact suggests that the processes of both introduction and ionisation are facilitated due to the release of active centres of the surface.

3. Electrochemical cleaning of the surface by means of quadruple potential cycling within a wide range of values contributes to the growth of the extraction rate constant from $3.29 \cdot 10^{-4}$ to $6.74 \cdot 10^{-4} \text{ cm/s}$.

Contribution of the authors

The authors contributed equally to this article.

Conflict of interests

The authors declare that they have no known competing financial interests or personal relationships that could have influenced the work reported in this paper.

References

1. Babak V. N., Didenko L. P., Kvurt Y. P., Sementsova L. A. Studying the operation of a membrane module based on palladium foil at high temperatures. *Theoretical Foundations of Chemical Engineering*. 2018;52(2): 181–194. <https://doi.org/10.1134/S004057951802001X>
2. Han Z., Xu R., Ningbo N., Xue W. Theoretical investigations of permeability and selectivity of Pd-Cu and Pd-Ni membranes for hydrogen separation. *International Journal of Hydrogen Energy*. 2021;46: 23715. <https://doi.org/10.1016/j.ijhydene.2021.04.145>
3. Liu J., Bellini S., Niek C. A. de Nooijer, ... Caravella A. Hydrogen permeation and stability in ultra-thin Pd-Ru supported membranes. *International*

Table 3. Parameters of hydrogen permeability obtained for samples 4 and 4'

Sample	Cathodic process				$K_D \cdot 10^9$, $\text{mol}/\text{cm}^2 \cdot \text{s}^{1/2}$
	Diffusion control		Phase boundary control		
	$D \cdot 10^8$, cm^2/s	$\Delta c_H \cdot 10^5$, mol/cm^3	$\bar{k} \cdot 10^4$, cm/s	$\Delta c_H \cdot 10^5$, mol/cm^3	
4	3.83 ± 0.11	2.48 ± 0.53	6.74 ± 1.41	1.02 ± 0.25	4.86 ± 1.02
4'	3.79 ± 0.18	1.41 ± 0.65	3.29 ± 1.23	0.55 ± 0.01	2.74 ± 0.84

- Journal of Hydrogen Energy*. 2020;45(12): 7455–7467. <https://doi.org/10.1016/j.ijhydene.2019.03.212>
4. Bosko M. L., Fontana A. D., Tarditi A., Cornaglia L. Advances in hydrogen selective membranes based on palladium ternary alloys. *International Journal of Hydrogen Energy*. 2021;46(29): 15572–15594. <https://doi.org/10.1016/j.ijhydene.2021.02.082>
 5. Endo N., Furukawa Y., Goshome K., Yaegashi S., Mashiko K., Tetsuhiko M. Characterization of mechanical strength and hydrogen permeability of a PdCu alloy film prepared by one-step electroplating for hydrogen separation and membrane reactors. *International Journal of Hydrogen Energy*. 2019;44(16): 8290–8297. <https://doi.org/10.1016/j.ijhydene.2019.01.089>
 6. Nooijer N., Sanchez J., Melendez J. Influence of H₂S on the hydrogen flux of thin-film PdAgAu membranes. *International Journal of Hydrogen Energy*. 2020;45 (12): 7303–7312. <https://doi.org/10.1016/j.ijhydene.2019.06.194>
 7. Lee Y-H., Jang Y., Han D. Palladium-copper membrane prepared by electroless plating for hydrogen separation at low temperature. *Journal of Environmental Chemical Engineering*. 2021;9(6): 106509. <https://doi.org/10.1016/j.jece.2021.106509>
 8. Yuna S., Oyama S. T. Correlations in palladium membranes for hydrogen separation: A review. *Journal of Membrane Science*. 2011;375(1-2): 28–45. <https://doi.org/10.1016/j.memsci.2011.03.057>
 9. Decaux C., Ngameni R., Solas D. Time and frequency domain analysis of hydrogen permeation across PdCu metallic membranes for hydrogen purification. *International Journal of Hydrogen Energy*. 2010;35(10): 4883–4892. <https://doi.org/10.1016/j.ijhydene.2009.08.100>
 10. Zhaoa P., Goldbacha A., Xu H. Low-temperature stability of body-centered cubic PdCu membranes. *Journal of Membrane Science*. 2017;542: 60–67. <http://dx.doi.org/10.1016/j.memsci.2017.07.049>
 11. Ievlev V. M., Roshan N. R., Belonogov E. K., ... Glazunova Yu. I. Hydrogen permeability of foil of Pd-Cu, Pd-Ru and Pd-In-Ru alloys received by magnetron sputtering. *Condensed Matter and Interphases*. 2012;14(4): 422–427. Available at: <https://www.elibrary.ru/item.asp?id=18485336>
 12. *Hydrogen in Metals* / Alefeld and J. Volkl (eds.). Berlin; New York: Springer-Verlag; 1978. V.2. 332 p.
 13. Morozova N. B., Vvedenskii A. V., Beredina I. P. The phase-boundary exchange and the non-steady-state diffusion of atomic hydrogen in Cu-Pd and Ag-Pd alloys. Part I. Analysis of the model. *Protection of Metals and Physical Chemistry of Surfaces*. 2014;50(6): 699–704. <https://doi.org/10.1134/S2070205114060136>
 14. Francia E. D., Lahoz R., Neff D., Caro T. D., Angelini E., Grassini S. Laser-cleaning effects induced on different types of bronze archaeological corrosion products: chemical-physical surface characterization. *Applied Surface Science*. 2022;573: 150884 <https://doi.org/10.1016/j.apsusc.2021.150884>
 15. Liu Y., Liu W. J., Zhang D. Experimental investigations into cleaning mechanism of ship shell plant surface involved in dry laser cleaning by controlling laser power. *Applied Physics A*. 2020;126: 866. <https://doi.org/10.1007/s00339-020-04050-y>
 16. Mao H., Fan W., Cao H., Chen X., Qiu M., Verweij H., Fan Y. Self-cleaning performance of in-situ ultrasound generated by quartz-based piezoelectric membrane. *Separation and Purification Technology*. 2022;282(B): 120031. <https://doi.org/10.1016/j.seppur.2021.120031>
 17. Chong W. Y., Secker T. J., Dolder P. N., The possibilities of using ultrasonically activated streams to reduce the risk of foodborne infection from salad. *Ultrasound in Medicine and Biology*. 2021;47(6): 1616–1630. <https://doi.org/10.1016/j.ultrasmedbio.2021.01.026>
 18. Zhang H., He F., Che Y., Song Y., Zhou M., Ding, D. Effect of annealing treatment on response characteristics of Pd-Ni alloy based hydrogen sensor. *Surfaces and Interfaces*. 2023;36: 102597 <https://doi.org/10.1016/j.surfin.2022.102597>
 19. Yin Z., Yang Z., Du M., ... Li S. Effect of annealing process on the hydrogen permeation through Pd–Ru membrane. *Journal of Membrane Science*. 2022;654: 120572 <https://doi.org/10.1016/j.memsci.2022.120572>
 20. Yang H., Tang Y., Zou S. Electrochemical removal of surfactants from Pt nanocubes. *Electrochemistry Communications*. 2014;38: 134–137. <https://doi.org/10.1016/j.elecom.2013.11.019>
 21. Pu H., Dai H., Zhang T. Metal nanoparticles with clean surface: The importance and progress. *Current Opinion in Electrochemistry*. 2022;32: 100927. <https://doi.org/10.1016/j.coelec.2021.100927>
 22. Uluc A. V., Moa J. M. C., Terryn H., Bottger A. J. Hydrogen sorption and desorption related properties of Pd-alloys determined by cyclic voltammetry. *Journal of Electroanalytical Chemistry*. 2014;734(15): 53–60. <https://doi.org/10.1016/j.jelechem.2014.09.021>
 23. Morozova N. B., Vvedenskii A. V. Phase-boundary exchange and non-stationary diffusion of atomic hydrogen in metal film. I. Analysis of current transient. *Condensed Matter and Interphases*. 2015;17(4): 451–458. <https://journals.vsu.ru/kcmf/article/view/91/194>
 24. Fedoseeva A. I., Morozova N. B., Dontsov A. I., Kozaderov O. A., Vvedenskii A. V. Cold-rolled binary palladium alloys with copper and ruthenium: injection and extraction of atomic hydrogen. *Russian Journal of Electrochemistry*. 2022;58(9): 812–822. <https://doi.org/10.1134/S1023193522090051>

Information about the authors

Natalia B. Morozova, Cand. Sci. (Chem.), Associate Professor, Department of Physical Chemistry, Voronezh State University (Voronezh, Russian Federation).

<https://orcid.org/0000-0003-4011-6510>
mnb@chem.vsu.ru

Lidiya E. Sidyakina, 2th year undergraduate student of the Department of Physical Chemistry, Voronezh State University (Voronezh, Russian Federation).

<https://orcid.org/0000-0001-6002-1434>
sidykina_lidia98@mail.ru

Alexey I. Dontsov, Cand. Sci. (Phys.–Math.), Associate Professor, Department of Materials Science and Industry of Nanosystems, Voronezh State University; Associate Professor of the Department of Physics, Voronezh State Technical University (Voronezh, Russian Federation).

<https://orcid.org/0000-0002-3645-1626>
dontalex@mail.ru

Vvedenskii Alexander V., Dr. Sci. (Chem.), Full Professor, Department of Physical Chemistry, Voronezh State University (Voronezh, Russian Federation).

<https://orcid.org/0000-0003-2210-5543>
alvved@chem.vsu.ru

Received 28.03.2023; approved after reviewing 03.04.2023; accepted for publication 15.05.2023; published online 25.09.2023.

Translated by Irina Charychanskaya